Biogeosciences Discuss., 5, 3409–3432, 2008
www.biogeosciences-discuss.net/5/3409/2008/

Biogeosciences Discussions

Biogeosciences Discussions is the access reviewed discussion forum of *Biogeosciences*

Carbonate precipitation by the thermophilic archaeon *Archaeoglobus fulgidus*: a model of carbon flow for an ancient microorganism

L. L. Robbins[1], K. A. Van Cleave[1], and P. Ostrom[2]

[1]US Geological Survey, St. Petersburg, FL, USA
[2]Department of Zoology, Michigan State University, East Lansing, MI, USA

Received: 10 July 2008 – Accepted: 18 July 2008 – Published: 28 August 2008

Correspondence to: L. L. Robbins (lrobbins@usgs.gov)

Published by Copernicus Publications on behalf of the European Geosciences Union.

Abstract

Microbial carbonate precipitation experiments were conducted using the archaeon bacteria *Archaeoglobus fulgidus* to determine chemical and isotopic fractionation of organic and inorganic carbon into mineral phases. Carbonate precipitation was induced in two different experiments using *A. fulgidus* to determine the relative abundance of organically derived carbon incorporated into carbonate minerals as well as to define any distinct phases or patterns that could be attributed to the precipitation process. One experiment used a medium containing ^{13}C-depleted organic carbon and ^{13}C-enriched inorganic carbon, and the other used a ^{14}C-labeled organic carbon source. Results indicated that 0.9–24.8% organic carbon was incorporated into carbonates precipitated by *A. fulgidus* and that this process was mediated primarily by pH and CO_2 emission from cells. Data showed that the carbon in the CO_2 produced from this microorganism is incorporated into carbonates and that the rate at which precipitation occurs and the dynamics of the carbonate precipitation process are strongly mediated by the specific steps involved in the biochemical process for lactate oxidation by *A. fulgidus*.

1 Introduction

It has long been recognized that microbes are capable of influencing mineralization processes, but the significant magnitude of microbial calcification in sediment deposition is only recently being realized. The difficulty in recognizing biogenic versus abiogenic minerals has been, in part, often due to similarities in morphologies and lack of unambiguous biomarkers. Understanding how cellular physiology affects calcification processes is one critical way of developing reliable geochemical tools for identification of microbial biomarkers in carbonates. Microbial influences on carbonate precipitation include a variety of processes, such as the inhibition of extracellular carbonate nucleation via biologically produced molecules, the enhancement of carbonate precipitation due to cell surface charge distribution, and the regulation of carbonate precipitation

BGD

5, 3409–3432, 2008

through the uptake or release of metabolic products (Sumner, 1997). For heterotrophic bacteria, nutritional conditions are a major factor in the relationships between crystals and bacteria (Castanier et al., 1999). The precipitation of carbonates has been demonstrated to occur on the cell surfaces of heterotrophic marine bacteria under both aerobic and anaerobic, agitated and non-agitated laboratory conditions, and at pHs ranging between 6.9 and 8.7 (Krumbein, 1974). Carbonate precipitation using a hyperthermophilic archaeon was demonstrated by Robbins et al. (1999) and Van Cleave (2003).

Archaeons are thought to be one of the most ancient forms of life to exist on Earth, appearing during the Archaean Era around 3.9 billion years ago. Recently, heterotrophic Archaea were found to dominate the sedimentary subsurface ecosystems off Peru (Biddle et al., 2006). These findings highlight how much is still to be learned about microbial processes in sediments.

Our experiments used *Archaeoglobus fulgidus*, a strictly anaerobic, hyperthermophillic archaeon which grows at temperatures between 60–95°C and at a pH range of 5.5–7.5, with optimal growth occurring at 83°C and pH of 6.9 (Stetter, 1988). *Archaeoglobus fulgidus* grows chemolithoheterotrophically through dissimilatory sulfate reduction and the complete oxidation of lactate to CO_2. *Archaeoglobus fulgidus* also fixes CO_2 in the presence of H_2 (Stetter, 1988). Significant for potentially influencing mineral precipitation by acting as a template, *A. fulgidus* cells consist of an S-layer composed of glycoprotein subunits in hexagonal array (Stetter, 1988).

Precipitation experiments using carbon isotopes were performed using *Archaeoglobus fulgidus* to construct a model for the production of carbonates and carbon transfer to the mineral phase. Of interest were the questions of whether microbially produced organic carbon and CO_2 derived from microbial metabolism are incorporated into the crystal, and if so, to what extent. In these experiments, carbonate precipitation was induced by *A. fulgidus* in medium containing ^{13}C-depleted organic carbon (isotopically light organic carbon) and a ^{13}C-enriched inorganic carbon in order to determine the relative percentage of inorganic:organic C in samples containing carbonate. Using [3–^{14}C] lactic acid as the primary source of carbon for the archaeon, we determined

whether CO_2 evolved from the oxidation of lactate by *A. fulgidus* was incorporated into precipitated carbonate minerals and helped to define distinct phases or patterns attributed to the precipitation process. This information provides insight into how closely linked the carbon cycle is coupled between microbial metabolism and mineral precipitation processes and provides some insight into mineral biomarkers.

2 Materials and methods

2.1 Culturing of *Archaeoglobus fulgidus*

One-milliliter aliquots of *A. fulgidus* cells obtained from the Deutsche Sammlung von Mikroorganismen und Zellkulturen GmbH (DSMZ German Collection of Microorganisms) were added to serum bottles containing 100 ml of *A. fulgidus* medium (Van Cleave, 2003) in 1-ml aliquots and incubated at 83°C for 5 days. SYBR Gold nucleic acid gel stain obtained from Molecular Probes™ was used to stain cells for direct counts. Cell concentrations of cultures in stationary phase after a 5-day incubation period ranged from 4.60×10^7 to 8.89×10^8 cells ml^{-1}.

2.2 Carbonate precipitation and isotope fractionation experiment

Precipitation medium (Van Cleave, 2003), created to facilitate precipitation of carbonate by *A. fulgidus*, was made using lactic acid with a $\delta^{13}C$ value of −22%, 99.9% ^{13}C-labeled sodium bicarbonate, and 99.9% ^{13}C-labeled CO_2. The medium was added in 500 ml aliquots to two 500 ml serum bottles pre-flushed with N_2 gas. The medium was subsequently reduced by adding 0.25 g of cysteine HCl to each serum bottle. Each serum bottle was gassed with $^{13}CO_2$to adjust the pH to 6.9. Approximately 1000 ml of *A. fulgidus* culture was centrifuged anaerobically under N_2 gas in twenty 50-ml centrifuge tubes for 15 min at 16 000×G. The supernatant was discarded from each tube, and the remaining pellets were re-suspended in 10-ml of precipitation medium and

immediately re-centrifuged. The supernatant was discarded from each tube, and the pellets were suspended in the reduced precipitation medium present in the two 500-ml serum bottles (10 pellets per bottle). The bottles containing the medium and cells were vortexed for 30 s. One hundred milliliter aliquots of medium containing the cells were added to ten 100 ml serum bottles, pre-flushed with nitrogen. The bottles were then incubated at 83°C. A single serum bottle was removed from the incubator at 0, 1, 2, 3, 4, 8, 12, 16, 20, and 24 h. Approximately 1 ml of medium and cells was extracted from the serum bottle for each time step, filtered though a 0.022 μm filter, and 2-ml of deionized water filtered, to remove any residual medium. The filter was then coated with gold palladium and analyzed using a Hitachi S-3500N scanning electron microscope (SEM). Carbonate and organic material was retrieved from each serum bottle according to the steps outlined in Fig. 1. Samples were then analyzed for ^{13}C values using a Thermo Finnigan Delta PLUS XL mass spectrometer. For pellets of combined organic material and carbonate, 20 to 40 μg of sample were used for each mass spectrometer analysis. For each pellet of organic material alone, 80 to 150 μg of sample was used for each mass spectrometer analysis. Cell counts were performed for each time step using a direct-count method with SYBR Gold staining.

The biomass, calculated using a 310 fg C μm^{-3} conversion factor (Fry, 1990), for each sample ranged from 2.07×10^{10} to 3.03×10^{9} fg C. The percentage of carbonate C and the percentage of organic C in sample OC for each time interval were determined using Eqs. (1) and (2).

$$\delta^{13}C_{sample} = f_1\delta^{13}C_1 + f_2\delta^{13}C_2 \quad (1)$$

$$f_1 + f_2 = 1 \quad (2)$$

where $\delta^{13}C_{sample}$=value for OC, f_1=fraction of organic C in OC (unknown), $\delta^{13}C_1$=value for organic C in OC f_2=fraction of carbonate C (unknown) in OC, and $\delta^{13}C_2$=value for carbonate C in OC.

The value of $1-f_1$ was assigned for f_2. The average δ^{13}C value of carbonates precipitated inorganically at 83°C from microbial precipitation medium made with 99.9%

^{13}C-labeled sodium bicarbonate and 99.9% ^{13}C-labeled CO_2 was used for $\delta^{13}C_2$ for each time step. The biomass for each time step was calculated using Eq. (3):

$$\text{Biomass} = (\pi/4)d^2(1-d/3)\times(\text{cells/ml}\times\text{ml of culture}) \text{ (Fry, 1990)}. \quad (3)$$

The value for d represents the average diameter of *A. fulgidus* cells for each time step. The diameter for each cell was measured from SEM images of cells captured at each time step.

2.3 ^{14}C experiment

In order to determine whether CO_2 evolved from the oxidation of lactate by *A. fulgidus* was incorporated into precipitated carbonate minerals, experiments were conducted using [3-^{14}C] lactic acid as the primary source of carbon for the archaeon. *Archeoglobus fulgidus* cells (1-ml aliquots) were added to serum bottles containing 100 ml of *A. fulgidus* medium and incubated at 83°C for 5 days. Two-hundred milliliters of two separate *A. fulgidus* cultures (1 and 2) in stationary phase were centrifuged anaerobically under N_2 gas in separate centrifuge tubes at 16 000×G for 15 min. The only difference between cultures 1 and 2 was cell count. The supernatant was discarded and the remaining microbial pellets were re-suspended into eight separate 100-ml serum bottles containing reduced *A. fulgidus* culture medium minus the yeast extract and sodium lactate components. Four of the bottles contained cells from culture 1, and four of the bottles contained cells from culture 2. Fifteen microliters of 57 mCi/mmol [3-^{14}C] lactic acid were added to each 100-ml bottle. The serum bottles were incubated for 4 days at 83°C. Following the 4-day incubation period, each bottle was spiked with an additional 7.5 µl of 57 mCi/mmol ^{14}C-labelled lactic acid and incubated for an additional 3 h. Following the second incubation period, the four serum bottles containing cells from culture 1 had a cell concentration of 1.27×10^7 cells ml^{-1}, whereas the four serum bottles containing the cells from culture 2 had a cell count of 1.09×10^8 cells ml^{-1}. The media and cells were then centrifuged anaerobically under N_2 gas in separate centrifuge tubes (two 50-ml tubes for each 100-ml serum bottle) at

BGD
5, 3409–3432, 2008

16 000×G for 15 min. The supernatant was discarded and each microbial pellet was rinsed in 15 ml of precipitation medium to remove any excess extracellular ^{14}C and re-centrifuged anaerobically at 16 000×G for 15 min. The supernatant was discarded from each tube, and the remaining microbial pellets were re-suspended into four separate 100-ml serum bottles (two pellets for each 100-ml bottle) containing 100 ml of reduced precipitation medium. The two bottles containing cells from culture 1 (samples A and B) had a cell count of 2.36×10^7 cells ml^{-1}, whereas the two bottles containing cells from culture 2 (samples C and D) had a cell count of 1.26×10^8 cells ml^{-1}. Samples A and B were incubated at 83°C for 200 h, and samples C and D were incubated at 83°C for 96 h. Every 8 h, a 1-ml aliquot was taken from each bottle and added to a scintillation vial. Ten milliliters of LCD cocktail was added, vortexed for 30 s, and subsequently analyzed using a TM Analytic 6891 Delta 300 liquid scintillation counter. Each vial was analyzed five times for 30 s.

3 Results

Figure 2 shows time-lapsed SEM images of the precipitation of carbonate by *Archaeoglobus fulgidus* cells over a 24-h period. From the onset of precipitation at 0 h to the final image captured after 24 h, the total size of cells and associated carbonate crystals increased from 250 nm in diameter to roughly 2.75 μm in diameter. Cell counts, average cell diameter, pH measurements, and calculated biomass for each time step over the 24-h duration of the experiment are reported in Table 1. Also shown in Table 1 are the $\delta^{13}C$ value for the organics+carbonate pellet (OC) and the pellet composed only of organics (O) as well as the percentage of organics and percentage of carbonate in the OC sample. The overall pH of the medium increased by 0.59 over the 24-h time period. Cell counts ranged from 2.77×10^7 to 3.60×10^7 cells/ml for each time step. The average cell diameter of *A. fulgidus* cells for each time step ranged from 230 nm to 500 nm. Figure 3 shows a graphical representation of the values for the log of the cell counts, the log of the biomass, the percentage of carbonate C in sample OC, the

BGD
5, 3409–3432, 2008

percentage of organic C in OC, and the pH of the medium over a 24-h period. Between 12 and 24 h, there is a negative correlation between the pH of the medium and the percentage of organic C in OC (r=−0.997) and a positive correlation between the pH and the percentage of carbonate C in OC (r=0.997), indicating that precipitation is driven by the pH of the medium.

Figure 4 shows the ^{14}C values, in disintegrations per minute (DPM), of the medium, cells, and carbonate for samples A, B, C, and D. Disintegration per minute values for the carbonate were above background ^{14}C levels for all four samples and showed distinct maximum values and minimum values. Values (DPM) for the total (supernatant, cells and carbonate) and the supernatant for samples A and B were significantly higher than the values for cells and carbonate, whereas DPM values for the total (supernatant, cells, and carbonate) were significantly higher than the values for cells, carbonate, and supernatant for samples C and D.

Carbonate, cell, supernatant, and total (cells, carbonate, and supernatant) values in Fig. 4 for samples A, B, C, and D show distinct patterns. These patterns were separated into three separate phases (I, II, and III). Phase I was characterized by cell, carbonate, total, and supernatant trends which were not in step with each other. During phase I, when the DPM values of cells and/or carbonate mineral were increasing or at a maximum, one or both supernatant values and the total were decreasing or at a minimum and vice versa. Phase I occurred for sample A (Fig. 4) between 16 and 56 h, 64 and 72 h, and 88 and 120 h, and 136 and 160 h; for sample B (Fig. 4) between 16 and 80 h, 104 and 112 h, and 136 and 160 h; for sample C (Fig. 4) between 0 and 16 h, 40 and 56 h, and 80–96 h; and for sample D (Fig. 4) between 0 and 32 h, 80 and 96 h, and 40–52 h. Phase II was characterized by cell, carbonate, supernatant, and total (cells, carbonate, and supernatant) and supernatant trends, which were all in step. Phase II occurred for sample A (Fig. 4) between 56 and 64 h, 120 and 128 h, and 144 and 160 h; for sample B (Fig. 4) between 88 and 96 h, and 112 and 136 h; for sample C (Fig. 4) between 16 and 32 h, and 72 and 80 h; and for sample D (Fig. 4) between 56 and 72 h. Phase III was characterized by cell and carbonate trends, which

BGD
5, 3409–3432, 2008

were matched and total (cells, carbonate, and supernatant) and supernatant trends, which were matched. However, the two pairs were not in phase with each other. In other words, when cell and carbonate trends increased or were at a maximum, total and supernatant trends decreased or were at a minimum and vice versa. In Fig. 4, phase III occurred for sample A between 72 and 88 h and 128 and 136 h; for sample B between 96 and 104 h; for sample C between 32 and 40 h and 56 and 72 h; and for sample D between 32 and 40 h and 72 and 88 h.

The three different phases (I, II, and III) observed in samples A, B, C, and D for the precipitation of ^{14}C carbonates occurred in a specific sequential order which is present in all four samples. At some point during the microbial-precipitation process, phase I, phase II, phase III, and phase I occurred in consecutive order for samples A, B, C, D. This sequence occurred between 88 and 144 h for sample A (Fig. 4), between 16 and 112 h for sample B (Fig. 4), between 0 and 56 h for sample C (Fig. 4) and between 40 and 96 h in sample D (Fig. 4).

4 Discussion

These experiments demonstrate that *Archaeoglobus fulgidus* plays a role in the precipitation of carbonate minerals and that a biological fingerprint is imparted on precipitated carbonate minerals through the incorporation of carbon in the form of CO_2. Results of ^{14}C experiments indicate that the process that *A. fulgidus* uses to incorporate CO_2 within the mineral phase occurs as it gains energy through dissimilatory sulfate-reduction and the oxidization of lactate to CO_2 (Stetter, 1988), according to the following equation (Möller-Zinkhan and Thauer, 1990):

$$CH_3CHOHCOO^- + 1.5SO_4^{2-} + 4H^+ \rightarrow 3CO_2 + 1.5H_2S + 3H_2O \quad (4)$$

The oxidation of lactate to $3CO_2$ proceeds via an acetyl-CoA/carbon monoxide dehydrogenase pathway, in which the second step is catalyzed by pyruvate: ferredoxin oxidoreductase (Kunow et al., 1995).

Möller-Zinkhan and Thauer (1990) performed experiments with [2-^{14}C] pyruvate, [3−^{14}C] pyruvate, and $^{14}CO_2$ to determine the distribution of carbon during lactate oxidation by *A. fulgidus*. It was determined that [2−^{14}C] pyruvate became decarboxylated to [1−^{14}C] acetyl CoA, while [3−^{14}C] pyruvate produced [2−^{14}C] acetyl CoA and released $^{14}CO_2$. When the assay was performed in the presence of $^{12}CO_2$, the acetyl CoA underwent an isotopic exchange with outside $^{12}CO_2$, releasing ^{14}C atoms and incorporating ^{12}C atoms into the methyl and carbonyl groups.

When the assay was performed by Möller-Zinkhan and Thauer (1990) in the presence of $^{14}CO_2$, ^{14}C-carbon atoms were exchanged with the acetyl CoA-carbon atoms and were incorporated into the methyl and carbonyl group in a specific ratio of 23% to 76%. The carbonyl group from the [1−^{14}C] acetyl CoA was converted to $^{14}CO_2$, indicating that 76% of the carbon incorporated into the acetyl CoA through isotopic exchange was released as a gas. No $^{14}CO_2$ was evolved during the conversion of [3−^{14}C] pyruvate to [2−^{14}C] acetyl CoA, indicating that the methyl group was not oxidized to CO_2during this step.

Our experiments using [3−^{14}C] lactic acid determined that CO_2 evolved from the oxidation of lactate by *A. fulgidus* was concomitantly incorporated into carbonate minerals. The Möller-Zinkhan and Thauer (1990) model was also used to help explain the dynamics of any salient patterns specific to the carbonate-precipitation cycle.

4.1 Model for carbonate precipitation – and incorporation of carbon into carbonate

One of the most important contributions of microorganisms to mineral precipitation is their role in catalyzing nucleation. It has been suggested that a microorganism in a saturated solution serves as a foreign solid that becomes a foundation or template for the development of nuclei (Fortin et al., 1997). The cell envelope of *Archaeoglobus fulgidus* consists of glycoprotein subunits forming an S-layer (Stetter, 1988). The S-layer is hexagonally patterned and forms a meshwork of open pores that promote highly efficient carbonate nucleation (Schultze-Lam et al., 1996). The S-layer is comprised of

exposed, identical reactive sites between carboxyl groups at the end of amino acids, to which divalent cations, Fe^{2+}, Mg^{2+}, Ca^{2+}, Mn^{2+}, Pb^{2} attach. The metal ions remain attached to the outer cell and form ionic bonds with CO_3^{2-} anions, resulting in carbonate mineral formation.

Our observations of carbonate precipitation on *A. fulgidus* cells for the first hour of induction experiments show the first solid-carbonate products to appear on the surface of the cells as patches, later to extend and coalesce to form a cocoon-like covering (Fig. 2) and are in close agreement with that of Castanier et al. (1999). These observations agree with the hypothesis proposed by Coleman (1993) that initial spheroidal carbonate formation is succeeded by a stage wherein the locus of precipitation moves beyond the previous boundary both laterally and vertically. However, the SEM images in Fig. 2 show that this phenomenon occurs a second time between 4 and 8 h and begins a third time after 8 h. After 12 h, carbonate formation no longer occurs in smooth, uniform sheets, but begins to form rapidly and sporadically. After 18 h, perfectly symmetrical, spheroidal carbonate shapes are no longer abundant, and the carbonates begin to take on the shapes of well-defined crystals that have reached sizes as large as 2.75 μm. This may indicate that between 9 and 15 h the majority of carbonate precipitation has become regulated by strictly inorganic processes, which would explain the transition from smooth symmetrical spheroids to almost angular crystals.

Figure 2 shows a step-wise progression of carbonate precipitation on the microbial cells, representing the most prevalent form of carbonate-covered cell present at that specific time step as well as the first appearance of that form in large numbers. After a 24-h period, four different forms of cells covered in carbonate (present throughout the 24-h precipitation sequence), including cells in the initial stages of carbonate nucleation, are present together in one small locality. This indicates that the rate of microbial precipitation occurs heterogeneously throughout the medium. Scanning Electron Microscopy of the carbonates precipitated by *A. fulgidus* cells after four days shows aggregates of individual calcified cells, and well-defined carbonate crystals growing off individual calcified cells. Also observed were calcified cells embedded in biofilm (not

BGD
5, 3409–3432, 2008

shown here) similar to biomineral aggregates observed by Castanier et al. (1999).

The calculated values for the percentage of organic C and the percentage of carbonate C present in each OC pellet for each time step (Table 1) correlate well with the SEM images in Fig. 2. The fraction of carbonate is extremely small for the first two hours, making up less than 0.008 of the sample at 2 h. The small percentage of carbonate C is representative of the small-scale nucleation seen in Fig. 2. An even smaller percentage of carbonate present at 2 h most likely represents the onset of metabolic activity by *A. fulgidus* cells following a lag phase. Cellular activity results in the production of CO_2 from the oxidation of lactic acid (Stetter, 1988) leading to the subsequent partial dissolution of carbonate associated with cells. The cell counts (Table 1), which show that a slight increase in the number of cells occurs between 2 and 3 h followed by a major increase in the number of cells at sometime between 3 and 4 h, also indicate a major increase in metabolic activity.

Following a lag phase, there is an exponential increase of bacteria coupled with the accumulation of metabolic end products, resulting in the accumulation of carbonate and bicarbonate ions in the medium and a pH increase that induces carbonate precipitation (Castanier et al., 1999). A major increase in cell numbers (Table 1), which occurs between 3 and 4 h, is accompanied by an increase in biomass and pH (Fig. 3). However, a major increase in the percentage of carbonate C in OC occurs just before 3 h and then decreases significantly between 3 and 8 h. This can be attributed to more substantial carbonate nucleation (as seen in Fig. 2) than that which occurred between 0 and 2 h and subsequent partial dissolution of carbonate due to CO_2 production. The production of CO_2 by *A. fulgidus* cells is represented by the decrease in pH that occurs between 4 and 12 h and could lead to dissolution. However, the continual increase in carbonate from 0 to 12 h (Fig. 2) indicates that the rate of carbonate precipitation between 0 and 12 h is greater than the rate of carbonate dissolution.

Between 12 and 24 h, there is an overall major increase in the percentage of carbonate C in OC. The r-value of 0.997 in Table 2 indicates a strong correlation between pH and the fraction of carbonate in the sample for this time interval. The p-value of 0.053

BGD
5, 3409–3432, 2008

is marginally high, most likely due to the low n-value. The p- and r-values for the 0 to 24-h time interval show a slightly weaker correlation between pH and the percentage of carbonate. However, no correlation exists between pH and the percentage of carbonate at the 0- to 4-h and 4- to 24-h time intervals. This indicates that pH does not play a major role in carbonate precipitation between 3 and 12 h. Therefore, the contribution of carbonate and bicarbonate ions to the medium through the oxidation of lactic acid by *A. fulgidus* has a more significant role in carbonate precipitation during this time interval than it does between 12 and 24 h. Cumulative H_2S production (raising pH) by *A. fulgidus* cells and cumulative CO_2 production between 3 and 12 h resulted in conditions ideal for substantial pH-mediated carbonate precipitation between 12 and 24 h. The perfectly symmetrical, spheroidal carbonate shapes observed between hours 1 and 9 may be the product of carbonate precipitation through increased bicarbonate saturation. However, angular carbonates observed between hours 9 and 24 are the product of predominately pH-mediated precipitation.

4.2 Cell incorporation of ^{14}C

The ^{14}C values for the cells varied throughout the duration of the experiment. When the ^{14}C values for *A. fulgidus* cells were at a maximum, the cells were in the process of converting [3–^{14}C] lactate into [3–^{14}C] pyruvate. When the ^{14}C values for the cells were at a minimum, the cells were at the end of the [3–^{14}C] lactate oxidation process. Because a large portion of the original ^{14}C in the [3–^{14}C] lactate had been evolved as $^{14}CO_2$ at this point, the ^{14}C values for the cells were lower than they were at the initiation of lactate oxidation. At the end of the lactate oxidation process, a small portion of the ^{14}C was incorporated into the cell while the rest was released as $^{14}CO_2$. Following the completion of the lactate oxidation process, the cells still had a ^{14}C signature from the incorporation of a portion of carbon from the methyl group of the [2–^{14}C] acetyl CoA into the cell. The mid-range ^{14}C values for the cells occurred when [3–^{14}C] pyruvate was being converted into [2–^{14}C] acetyl CoA. The acetyl CoA decarbonylase/synthase (ACDS) multienzyme complex catalyzed the synthesis of acetyl CoA according to the

reaction (Dai et al., 1998):

$$CO_2 + 2Fd_{red}(Fe^{2+}) + 2H^+ + CH_3{-}H_4SPt + CoA \rightarrow \text{acetyl CoA} + H_4SPt + 2Fd_{ox}(Fe^{3+}) + H_2O$$

where Fd is ferredoxin, and $CH_3{-}H_4SPt$ and H_4SPt denote N^5-methyl-tetrahydrosarcinapterin and tetrahydrosarcinapterin.

This reaction shows that ambient CO_2 is fixed during the formation of acetyl CoA. The fixed carbon dioxide is present as either $^{14}CO_2$ or $^{12}CO_2$. Mid-range ^{14}C values for the cells occur when the $^{14}CO_2$ is fixed and when the carbonyl and methyl groups in the [2−^{14}C] acetyl CoA undergo an isotopic exchange with outside $^{14}CO_2$. These ^{14}C values are not as high as those which occur during the conversion of [3−^{14}C] lactate to [3−^{14}C] pyruvate because a portion of ^{14}C in the lactate has left the cell as $^{14}CO_2$. Furthermore, ambient $^{12}CO_2$ incorporated into the methyl group of the acetyl CoA dilutes the ^{14}C signal.

4.3 Incorporation of ^{14}C into carbonate

Increases and decreases in carbonate trends represent an increase or decrease in the overall amount of ^{14}C present in carbonate minerals. The relatively high ^{14}C values for the carbonate fraction of samples A, B, C, and D indicate that ^{14}C derived from the oxidation of [3−^{14}C] lactic acid by *A. fulgidus* cells is incorporated into the microbially precipitated carbonates. In this process, [3−^{14}C] lactic acid is converted to [3−^{14}C] pyruvate and the [3−^{14}C] pyruvate produces $^{14}CO_2$as it is converted into [2−^{14}C] acetyl CoA. A mixture of $^{14}CO_2$and $^{12}CO_2$is produced as the carbonyl group in the acetyl CoA is reduced. A significant amount of $^{14}CO_2$ is also produced during the final step of oxidation of the methyl group in the [2−^{14}C] acetyl CoA. Some of the $^{14}CO_2$evolved during the lactate oxidation process is incorporated into carbonate minerals as $^{14}CO_3^{2-}$ while the remaining portion is either incorporated into the medium as ($H^{14}CO_3^-$) (Coleman, 1993) or remains in the gaseous form.

4.4 Supernatant and total (cells, carbonate, and supernatant)

Although cells grown on [3−^{14}C] lactic acid were rinsed prior to re-suspension in the precipitation medium, it is possible that some unoxidized [3−^{14}C] lactic acid bound to cells was not completely removed. This [3−^{14}C] lactic acid is therefore possibly present in the supernatant for samples A, B, C, and D. Fluctuations in ^{14}C values of the supernatant reflect changes in the amount of ^{14}C in the system present as $H^{14}CO_3^-$ and unoxidized [3−^{14}C] lactic acid not associated with cells. Increases and maximum ^{14}C values, which occur in supernatant trends, indicate an increase in the amount of ^{14}C present as $H^{14}CO_3^-$, whereas decreases and minimums represent a decrease in either [3−^{14}C] lactic acid, $H^{14}CO_3^-$, or both. The ^{14}C values for the total (includes cells, carbonate and supernatant) indicate the overall amount of ^{14}C present as a mixture of $^{14}CO_3^{2-}$, $H^{14}CO_3^-$,[3-^{14}C] lactic acid, and cellular material. Only a very small amount of $^{14}CO_2$ is represented in the ^{14}C values for the total because the majority of the gas is evolved during sample preparation for analysis.

In samples A and B (Fig. 4), the ^{14}C values for the total (cells, supernatant, and carbonate) and supernatant alone decrease significantly between 0 and 16 h and progressively decrease between 56 and 160 h. This can be attributed to a shift in the allocation of ^{14}C in the system as [3−^{14}C] lactic acid in the medium is oxidized and ^{14}C is incorporated into the medium as $H^{14}CO_3^-$, cellular material, and carbonates, or escapes as $^{14}CO_2$ gas. In samples C and D, the values for the cells, carbonate, and supernatant are lower than the value for the total (cells, carbonate, and supernatant). This is primarily due to the loss of $^{14}CO_2$(from cellular activity and outgassing), which occurs in the time period between sample extraction and the point at which cells are separated from carbonate. The value for the carbonate fraction in samples A, B, C, and D is the lowest of the four components because it is formed from both ambient $^{12}CO_2$ as well as $^{14}CO_2$ released during the conversion of [3−^{14}C] pyruvate to [2−^{14}C] acetyl CoA.

BGD
5, 3409–3432, 2008

5 Phases present during carbonate precipitation:

5.0.1 Phase I

Three different phases of precipitation/dissolution occurred during the experiment, often in sequential order. In phase I, carbonate, total (cell, carbonate, and supernatant), cell and supernatant data indicate that carbonate formation is mediated primarily by the production of $^{14}CO_2$ by *Archaeoglobus fulgidus*. When the ^{14}C values for the cells are at a maximum, the carbonate ^{14}C values are either decreasing or at a minimum. This indicates that the overall pH of the medium is not high immediately following $^{14}CO_2$ emission from the cells. When the ^{14}C values for the supernatant are increasing or at a maximum, $^{14}CO_2$ produced by *A. fulgidus* cells is incorporated into the medium as $H^{14}CO_3^-$. At this point, the pH of the medium is not high enough for carbonate precipitation to occur.

However, subsequently, when cell ^{14}C values are decreasing or at minimum values, the carbonate ^{14}C values are increasing or at a maximum and $^{14}CO_2$ has been generated to reach a carbonate saturation state sufficiently high for mineral formation. However, when the lactate oxidation process starts again, $^{14}CO_2$ released during the early stages of [3–^{14}C] lactate oxidation dissolves pre-existing carbonate. Carbonate is not re-precipitated until the ^{14}C values for the cells are at mid-range or low values.

5.0.2 Phase II

Once cell, carbonate, total (cells, carbonate, and supernatant), and supernatant trends are all in phase, the ^{14}C values for carbonate and the cells increase and decrease together, and the pH of the medium is high enough for carbonate precipitation to occur immediately following $^{14}CO_2$ release from *A. fulgidus* cells. The ^{14}C values for the supernatant also increase and decrease in phase with the values for the cells and carbonate fractions. Any non-oxidized [3–^{14}C] lactate (not associated with cells) present in the medium is masked at this time by the amount of $H^{14}CO_3^-$ or carbonic acid having

been introduced into the medium via $^{14}CO_2$ production from the oxidation of [3–^{14}C] lactate. Additionally, the data indicate that the rate at which $^{14}CO_2$ emitted from cells is incorporated into the medium as $H^{14}CO_3^-$ is proportional to the rate at which $^{14}CO_2$ is incorporated into carbonate minerals.

5.0.3 Phase III

In phase III, cell trends and carbonate trends are in phase, and total (cells, carbonate, and supernatant) trends and supernatant trends are in phase, but the two pairs are not in phase with respect to each other. This indicates that the ^{14}C in the system is predominately present as $H^{14}CO_3^-$. In phase III, when carbonate trends increase or are at a maximum, total trends decrease or are at a minimum, indicating that the amount of ^{14}C present as carbonate mineral and cells is significantly less than the ^{14}C present as $H^{14}CO_3$. Cells are at mid-range ^{14}C values, indicating that they are in the process of converting [3–^{14}C] pyruvate into [2–^{14}C] acetyl CoA. The $^{14}CO_2$ gas released from this process may be dissolving carbonate, resulting in lower carbonate ^{14}C values and higher supernatant ^{14}C values. The isotopic exchange with outside $^{12}CO_2$and production of lighter $^{12}CO_2$, which also occurs during this process, may also explain the lower ^{14}C values of any new carbonate precipitated.

5.1 Proposed model of carbonate precipitation

The phases (I, II, III, and I) observed in samples A, B, C, and D occur sequentially during carbonate precipitation by *A. fulgidus*. Further, the rate at which precipitation occurs and the dynamics of the carbonate precipitation process are strongly mediated by the specific steps involved in the biochemical process for lactate oxidation by *A. fulgidus*.

Phase I represents the initial step, in which carbonate precipitation occurs heterogeneously and sporadically and carbonates are continuously precipitated, dissolved, and re-precipitated. In phase I, carbonate precipitation is driven solely by $^{14}CO_2$ production from cells since overall pH of the medium has not increased. However, by phase

II, maximum of carbonate precipitation is occurring as a result of the overall pH of the medium increasing from dissimilatory sulfate-reduction. Phase III represents the transitional phase back to Phase I, in which the pH of the medium decreases from increased $^{14}CO_2$ production, but the majority of ^{14}C in the medium is still present as $H^{14}CO_3^-$. Complete repetition of all phases was not observed within the time frame of the experiment. However, we suggest that it is likely mediated by $H^{14}CO_3^-$ concentration and pH.

Acknowledgements. We gratefully acknowledge the help of the following individuals: K. Yates, D. Griffin, J. Lisle, C. Kellogg, J. Harwood, and A. Lapaglia; D. Hollander for his assistance with the mass spectrometer; J. Ryan for his assistance with the XRD; and T. Greco for his assistance with the SEM. This research was funded by the NASA Astrobiology Institute and the US Geological Survey.

References

Biddle, J. F., Lipp, J. S., Lever, M. A., Lloyd, K. G., Sorensen, K. B., Anderson, R., Fredricks, H. F., Elvert, M., Kelly, T. J., Scrag, D. P., Sogin, M. L., Brenchley, J. E., Teske, A., House, C. H., and Hinrichs, K.: Heterotrophic Archaea dominate sedimentary subsurface ecosystems off Peru, P. Natl. Acad. Sci. USA, 104(10), 3846–3851, 2006.

Castanier, S., Mètayer-Levrel, G., and Perthuisot, J.: Ca-carbonates precipitation and limestone genesis – the microbiogeochemist point of view, Sediment. Geol., 126, 9–23, 1999.

Coleman, M. L.: Microbial processes: controls on the shape and composition of carbonate concretions, Mar. Geol., 113, 127–140, 1993.

Dai, Y.-R., Reed, D. W., Millstein, J. H., Hartzell, P. L., Grahame, D. A., and Demoll, E.: Acetyl-CoA decarbonylase/synthase complex from *Archaeoglobus fulgidus*, Arch. Microbiol., 169, 525–529, 1998.

Fortin, D., Ferris, F. G., and Beveridge, T. J.: Surface-mediated mineral development by bacteria, Rev. Mineralogy, 35, 161–180, 1997.

Fry, J. C.: Direct methods and biomass estimation, Method Microbiol., 22, 42–85, 1990.

Krumbein, W. E.: On the precipitation of aragonite on the surface of marine bacteria, Naturwissenschaften, 61, 167, 1974.

Kunow, J., Linder, D., and Thauer, R. K.: Pyruvate: ferredoxin oxidoreductase from sulfate-reducing *Archaeoglobus fulgidus*: molecular composition, catalytic properties, and sequence alignments, Arch. Microbiol., 163, 21–28, 1995.

Möller-Zinkhan, D. and Thauer, R. K.: Anaerobic lactate oxidation to $3CO_2$ by *Archaeoglobus fulgidus* via the carbon monoxide dehydrogenase pathway: demonstration of the acetyl-CoA carbon-carbon cleavage reaction in cell extracts, Arch. Microbiol., 153, 215–218, 1990.

Robbins, L. L, Van Cleave, K., and Ryan, J.: Comparison of carbonate textural features in ALH84001 and microbially induced textures in orthopyroxene, Lunar and Planetary Science Conference XXX, 15–19 March 1999, Houston, Texas, 1464, 1999.

Schultze-Lam, S., Fortin, D., Davis, B. S., and Beveridge, T. J.: Mineralization of bacterial surfaces, Chem. Geol., 132, 171–181, 1996.

Stetter, K. O.: *Archaeoglobus fulgidus* gen. Nov., sp. Nov.: a New Taxon of extremely Thermophilic Archaebacteria, Syst. Appl. Microbiol., 10, 172–173, 1988.

Sumner, D. Y.: Late Archean calcite-microbe interactions: two morphologically distinct microbial communities that affected calcite nucleation differently, PALAIOS, 12, 302–318, 1997.

Van Cleave, K. A.: Archeon biomineralization in extreme environments and its implication of ancient carbonate fossils on earth and Mars, M.S. Thesis, University of South Florida, USA, 132 pp., 2003.

Table 1. Data obtained from 24-h carbonate precipitation experiment using *Archaeoglobus fulgidus* cells in a precipitation media prepared w/ isotopically light lactic acid and ^{13}C-enriched sodium bicarbonate and CO_2.

Time (h)	pH	Avg. cell count (cells/ml)	Avg. cell diameter (μm)	Biomass (fg C)	Avg. δ^{13}C value for OC[a]	Avg. δ^{13}C value for O[b]	% Organic C in OC	% Carbonate C in OC
0	6.92	3.28×10^{7}	0.36	1.28×10^{10}	+693.83‰	−24.55	97.2	2.8
1	6.94	2.77×10^{7}	0.31	7.00×10^{9}	+745.30‰	−25.61	97.0	3.0
2	6.95	2.80×10^{7}	0.30	6.38×10^{9}	+197.52‰	−26.16	99.1	0.9
3	7.00	2.99×10^{7}	0.33	8.79×10^{9}	+5974.55‰	−25.42	76.5	24.5
4	7.35	4.76×10^{7}	0.33	1.43×10^{10}	+3802.10‰	−24.11	85.0	15.0
8	7.27	3.76×10^{7}	0.34	1.22×10^{10}	+808.47‰	−19.22	96.8	3.2
12	7.02	2.09×10^{7}	0.50	2.07×10^{9}	+2274.40‰	−18.48	91.0	9.0
16	7.10	2.80×10^{7}	0.38	1.21×10^{10}	+1248.20‰	−19.36	95.0	5.0
20	7.50	3.12×10^{7}	0.23	3.03×10^{9}	+6316.11‰	−12.84	75.2	24.8
24	7.51	3.60×10^{7}	0.27	5.51×10^{9}	+5959.50‰	−26.16	76.6	23.4

[a] OC=Pellet comprised of carbonate and organic material
[b] O=Pellet comprised of organic material only

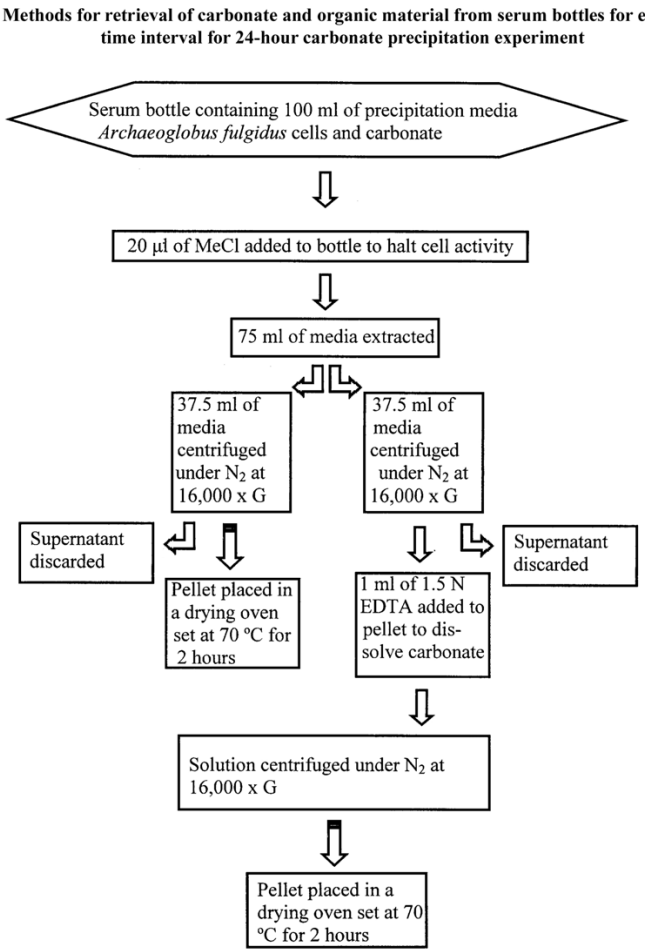

Fig. 1. Flow chart of methods.

BGD
5, 3409–3432, 2008

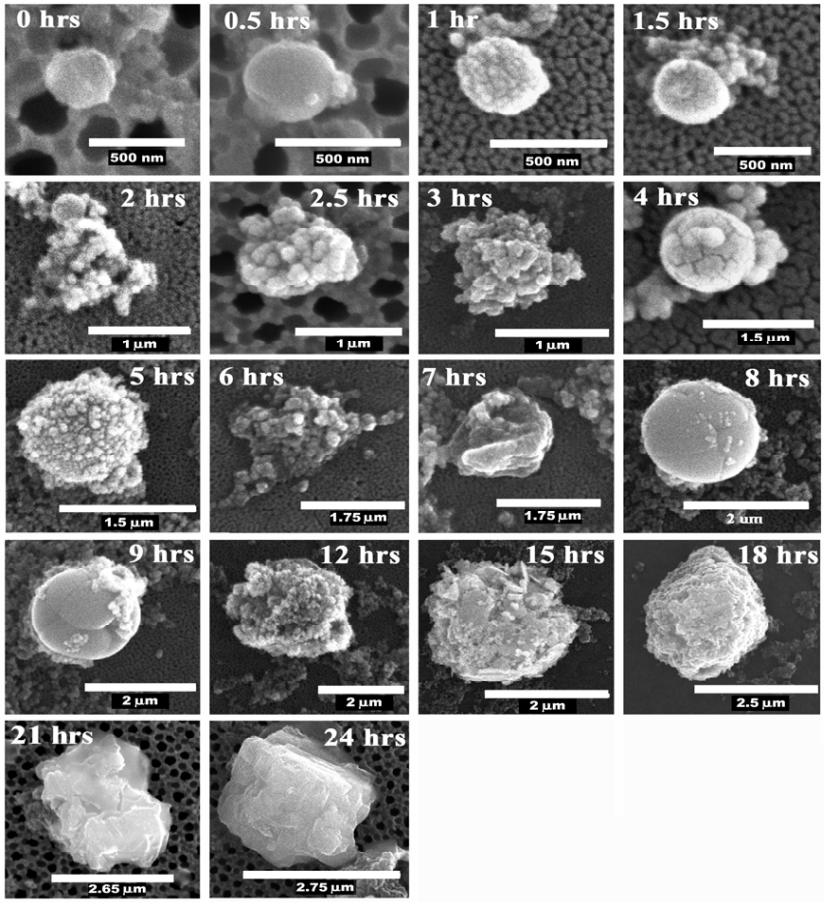

Fig. 2. Time-lapsed SEM images of carbonate precipitation by *Archaeoglobus fulgidus* cells over a 24-h period.

BGD

5, 3409–3432, 2008

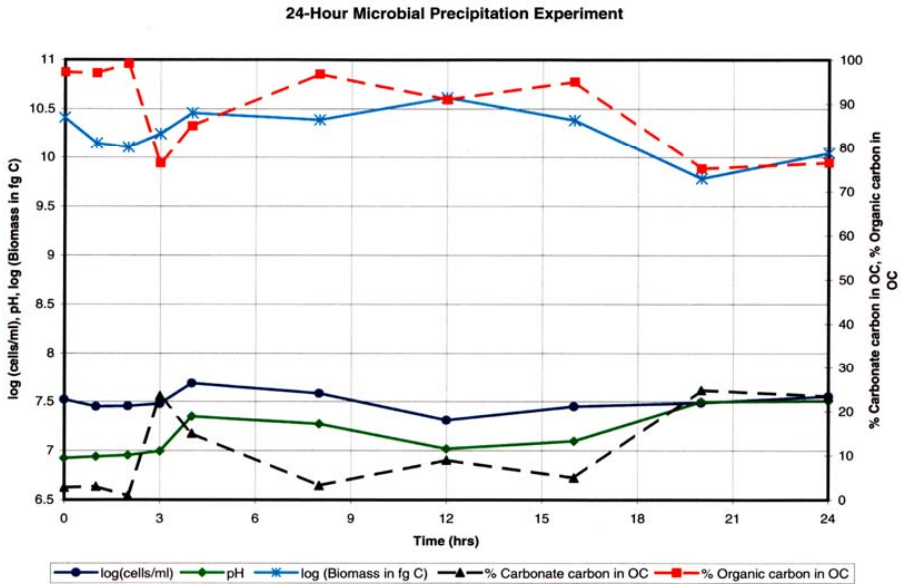

Fig. 3. Graphical representation of 24-h carbonate precipitation experiment using *Archaeoglobus fulgidus* cells. The red line represents the percentage organic carbon in the pellet (centrifuged out of solution in each serum bottle for each time step) comprised of carbonate and organic material (OC) for each time step. The black line represents the percentage of carbonate carbon in OC. The green line represents the measured pH for each time step. The dark blue line represents the log of the cell count for each time step (in cells/ml). The light blue line represents the log of the calculated biomass (in fg C) for each time step.

BGD
5, 3409–3432, 2008

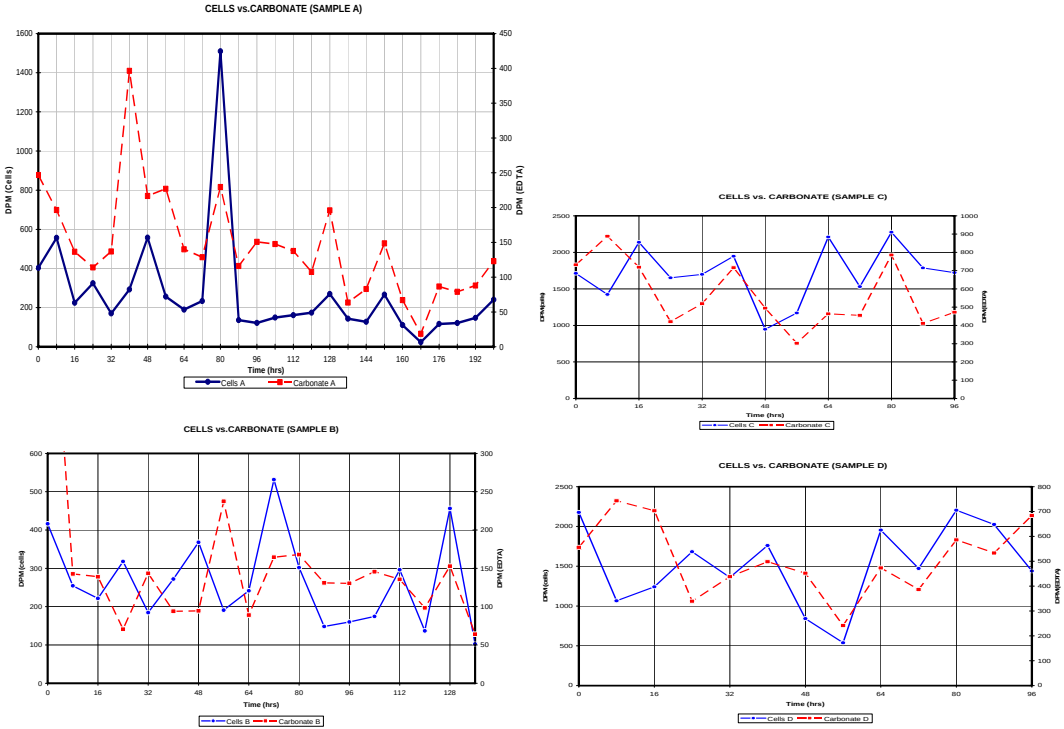

Fig. 4. Graphs of time series of samples **A, B, C, D** showing cell C (in DPM) vs. carbonate (in DPM).

BGD

5, 3409–3432, 2008